Supplement of

Modelling the artificial forest (*Robinia pseudoacacia* L.) root-soil water interactions in the Loess Plateau, China

Hongyu Li, Yi Luo, Lin Sun, Xiangdong Li, Changkun Ma, Xiaolei Wang, Ting Jiang, Haoyang Zhu

Correspondence to: Yi Luo (luoyi@igsnrr.ac.cn)

1. Ecohydrological model description

In this section, brief description of ecohydrological model have been presented, including biological components and hydrological components.

1.1 Biological components

1.1.1 Phenology

Phenological development of the plant is based on daily heat unit accumulation, computed as (Williams et al., 1989):

$$HU = T_{avg} - T_{base},\ when\ T_{avg} > T_{base} \quad \text{(S1)}$$

where *HU*, T_{avg} and T_{base} are the values of heat units, daily average temperature (°C), and the plant-specific base temperature in (°C). It is assumed that no growth occurs below the base temperature. A heat unit index (*HUI*) ranging from 0 at planting to 1 at physiological maturity is computed as follows.

$$HUI = \frac{\sum_i^m HU}{PHU} \quad \text{(S2)}$$

PHU is the potential heat units required for maturity of plant. If *HUI* exceeds 1, plant start to grow. Date of harvest, leaf area growth and senescence are affected by *HUI*.

1.1.2 LAI development

The *LAI* controls the precipitation interception, radiation absorption and transpiration. LAI development is estimated by the method according to the EPIC crop growth module (Williams et al., 1989), which could be expressed as:

$$LAI_i = LAI_{i-1} + \Delta LAI_i \quad \text{(S3)}$$

$$\Delta LAI_i = \left(fr_{LAImx,i} - fr_{LAImx,i-1}\right) \cdot LAI_{max} \cdot (1 - \exp\left(5(LAI_{i-1} - LAI_{max})\right)) \cdot \sqrt{REG_i} \quad \text{(S4)}$$

where LAI_i and LAI_{i-1} are the *LAI* values (m^2 m^{-2}) on day *i* and *i-1*, respectively; ΔLAI_i is the actual *LAI* increment on day *i*, $fr_{LAImx,i}$ and $fr_{LAImx,i-1}$ are the fractions of the plant's maximum *LAI* on day *i* and *i-1*, respectively; LAI_{max} is the maximum *LAI*, and REG_i is the stress factor combined with water and temperature on day *i* discussed in more detail below. LAI_{max} can be estimated using observation values.

1.1.3 Biomass accumulation and allocation

The daily synthesis of assimilates is calculated based on the intercepted photosynthetically active radiation and radiation use efficiency (Neitsch et al., 2011):

$$\Delta Bio = IPAR \cdot RUE \quad \text{(S5)}$$

where ΔBio is the photosynthetic assimilates for the increase of total plant biomass (kg m^{-2}). $IPAR$ is the amount of intercepted solar radiation by plant leaves (MJ m^{-2}), RUE is the radiation-use efficiency of the plant (kg MJ^{-1}).

The interception of solar radiation by plant canopy is calculated using Beer's law:

$$IPAR = 0.5 \cdot H_{day} \cdot (1 - \exp(-k_n LAI)) \quad \text{(S6)}$$

where k_n is the PFT dependent light extinction coefficient, H_{day} is the incident total solar radiation (MJ m^{-2}).

The radiation-use efficiency is determined by Jarvis-type approach, based on the basic photosynthetic physiological properties (e.g., carboxylation rate), and stresses of external factors like soil moisture and atmospheric temperature. Here, radiation-use efficiency is calculated by:

$$RUE_i = RUE_{max} \cdot REG_i \quad \text{(S7)}$$

where RUE_{max} is the maximum radiation-use efficiency for the plant (kg MJ^{-1}).

After assimilates are calculated, the next step is to allocate it to different carbon pools. In the Biome-BGC model, allocation ratio is assumed as constant. According to the relevant work on Biome-BGC simulation for black locust of Loess Plateau (Zhang et al., 2015), the fraction of biomass allocated for the roots to the total was about 0.3, and two ratios of coarse root pool and fine root pool to the new leaf biomass as 0.5 and 1.0, respectively. Therefore, 0.2 was set as the initial fraction value of total assimilates allocating to the fine roots. Afterwards, in the dynamic fine root distribution and rooting depth approach dynamic, newly assimilated biomass allocated to the fine roots ΔFR and the coarse roots ΔCR were updated at every time step.

1.2 Hydrological components

1.2.1 Soil water dynamics

The movement of soil water in the vadose zone can be described by Richards' equation (RE) (Richards, 1931) and a sink term is included to describe uptake or release by plant roots. In our study, a modified form of the θ-based RE with the hydrostatic pressure subtracted are used (Zeng and Decker,

2009), expressed as follows,

$$\frac{\partial \theta}{\partial t} = \frac{\partial}{\partial z}\left[K\left(\frac{\partial(\psi-\psi_E)}{\partial z}\right)+1\right] - Q_{root} \quad \text{(S8)}$$

where θ is the volumetric soil water content (mm3 mm-3), t is time (s), z is the vertical coordinate (mm, positive upwards), K is the hydraulic conductivity (mm s-1), ψ is the soil matric potential (mm), and z also represents the gravitational potential as used in the hydraulic potential $\psi + z$, ψ_E is the soil matric potential of the hydrostatic equilibrium state (mm). Power function have been used for representing the moisture characteristics (Campbell, 1974; Clapp and Hornberger, 1978), as it could provide sufficient numerical accuracy and acceptable computational expense (Shao and Irannejad, 1999):

$$K = K_{sat}\left(\frac{\theta}{\theta_{sat}}\right)^{2B+3} \quad \text{(S9)}$$

$$\psi = \psi_{sat}\left(\frac{\theta}{\theta_{sat}}\right)^{-B} \quad \text{(S10)}$$

The exponent *B* is calibrated according to the soil water observation.

The numerical solution is Thomas algorithm, which is referenced from CLM. Its detail description is thoroughly documented in the technical book of CLM (Oleson et al., 2013). As RE is a highly nonlinear, multiple smaller time steps is required to solve this equation. RE is solved at the hourly time step and then averaged for the daily condition.

Based on the soil properties and the topography of the site, the lateral movement of soil water was assumed to be negligible. Also, the observation of nearby runoff plots showed that no significant runoff occurred during the study period due to the high canopy cover during the raining season. Therefore, it is reasonable to describe the site soil water dynamics by 1-D RE and the upper boundary condition by the atmospheric boundary determined by rainfall, interception, and evapotranspiration.

1.2.2 Root water uptake

Root water uptake Q_{root} distributed over the soil layers proportionally to their fine root biomass and was locally controlled according to soil water (Simunek and Hopmans, 2009). Thus, root water uptake is calculated as follows:

$$Q_{root} = \sum_i^n QR_i \quad \text{(S11)}$$

$$QR_i = TR_a \cdot \frac{REW_i \cdot fr_i}{\sum_i REW_i \cdot fr_i} \quad \text{(S12)}$$

where Q_{root} is the total plant root water uptake (mm), QR_i is the root water uptake (mm) for the soil layer *i*.

1.2.3 Evapotranspiration

Potential evapotranspiration (ET_p, mm d^{-1}) is partitioned between the canopy (T_p, potential transpiration) and soil (E_p, potential evaporation).

The potential evapotranspiration of the site on day *i* is calculated from reference evapotranspiration ET_0 using the Penman–Monteith equation based on meteorological data (Allen et al., 1998). After calculating the ET_p, the canopy potential transpiration (T_p, mm d^{-1}) can be expressed as:

$$T_p = ET_p \cdot (1 - \exp(-k_n \cdot LAI)) \quad \text{(S13)}$$

where k_n is the light extinction coefficient.

In this study, temperature and soil water were considered to account for the effects of environmental

stress on transpiration. Then the actual transpiration (TR_a, mm d^{-1}) is calculated as:

$$REG = (1 - WStrs) \cdot (1 - TStrs) \quad \text{(S14)}$$

$$TR_a = T_p \cdot REG \quad \text{(S15)}$$

where $WStrs$ is water stress factor, and $TStrs$ is temperature stress factor.

The temperature stress factors calculation methods is based on SWAT (Neitsch et al., 2011), calculated as follow:

$$TStrs = \begin{cases} 1 & , \quad T_{avg} \le T_b, T_{avg} \ge T_m \\ 1 - exp\left[\frac{-0.0154(T_o - T_{avg})^2}{(T_o - T_b - abs(T_{avg} - T_o))^2}\right], & T_b < T_{avg} < T_m \end{cases} \quad \text{(S16)}$$

where T_{avg} is the mean temperature for day (℃), T_b is the plant' base or minimum temperature for growth (℃), and T_o is the plant's optimal temperature for growth (℃).

The water stress is represented as a smooth S-shape function (Sun et al., 2011; Yang et al., 2012):

$$WStrs = \frac{1}{1 + (REW/h_{REW})^{-k_{REW}}} \quad \text{(S17)}$$

where h_{REW} is the soil water content at which transpiration is halved. when REW is the value of h_{REW}, $WStrs$ = 0.5. k_{REW} is the shape coefficient, and larger k_{REW} value indicates a more rapid decline feature.

Finally, the actual soil evaporation E_{soil} is calculated by considering the soil moisture availability in the soil profile. In this study, soil evaporation is assume occurring in the top-most soil layer (Neitsch et al., 2011).

2. Literature data

(1) Literature data about fine root distribution has been synthetized from eight relating observational studies. These studies observed the fine root distributions of black locust plantations located in the southern part of the Loess Plateau (Zhao et al., 2000; Li et al., 2002; Xue et al., 2003; Li et al., 2005; Cao et al., 2006; Chen et al., 2009; Hu et al., 2010; Zhang et al., 2018a). The sampling details (e.g., locations, stand age, sampling) were presented in **Supplementary Excel File (*Literature data.xlsx*)**. These observations were undertaken by soil coring method and mainly distributed in the 0-2 m soil layer. All data (including biomass density, surface area density and length density) has been normalized into cumulative root distribution (%) along the soil profile. Finally, 15 columns of records were available.

(2) Literature data about maximum rooting depth of black locust from different stand age have been obtained from the dataset of Fan et al. (2017), which compiled rooting depth observations from multi-source reports worldwide. Finally, 3 groups of records about black locust forest were available.

(3) Literature data about deep profile of soil water content from black locust forestland from different sites in Loess Plateau stand age have been obtained from three papers (Li et al., 2008; Jia et al., 2017; Wu et al., 2021). Detailed values see in **Supplementary Excel File**. To quantify the degree of soil desiccation and comparison, soil desiccation index (SDI) is used. According to Wang et al. (2011), SDI is calculated as follows:

$$SDI = \frac{SW - WP}{SFC - WP} \quad \text{(S18)}$$

where SW is soil water content, WP is wilting point, and SFC is stable field capacity. In practice, soil water content at 60% of field capacity can be assumed to be the stable field capacity for the loess in the Loess Plateau. Soil desiccation intensity was divided into six grades based on SDI (Li et al., 2008):

(i) not desiccated if SDI ≥ 1; (ii) slightly if 0.75 ≤ SDI < 1; (iii) medium if 0.5 ≤ SDI < 0.75; (iv) seriously if 0.25 ≤ SDI < 0.5; (v) strongly if 0 ≤ SDI < 0.25); (vi) extremely if SDI < 0. Dried soil layer thickness (DSLT, cm) was calculated using the following equation (Wang et al. 2011):

$$DSLT = 20 \times \sum_i^n S(SW_i - SFC_i) \quad \text{(S19)}$$

Where $S(SW_i - WP_i) = \begin{cases} 0, & SW_i - SFC_i > 0 \\ 1, & SW_i - SFC_i > 0 \end{cases}$, (i = 5, 6, …, n). n = 25 (calculating soil depth of 500 cm).

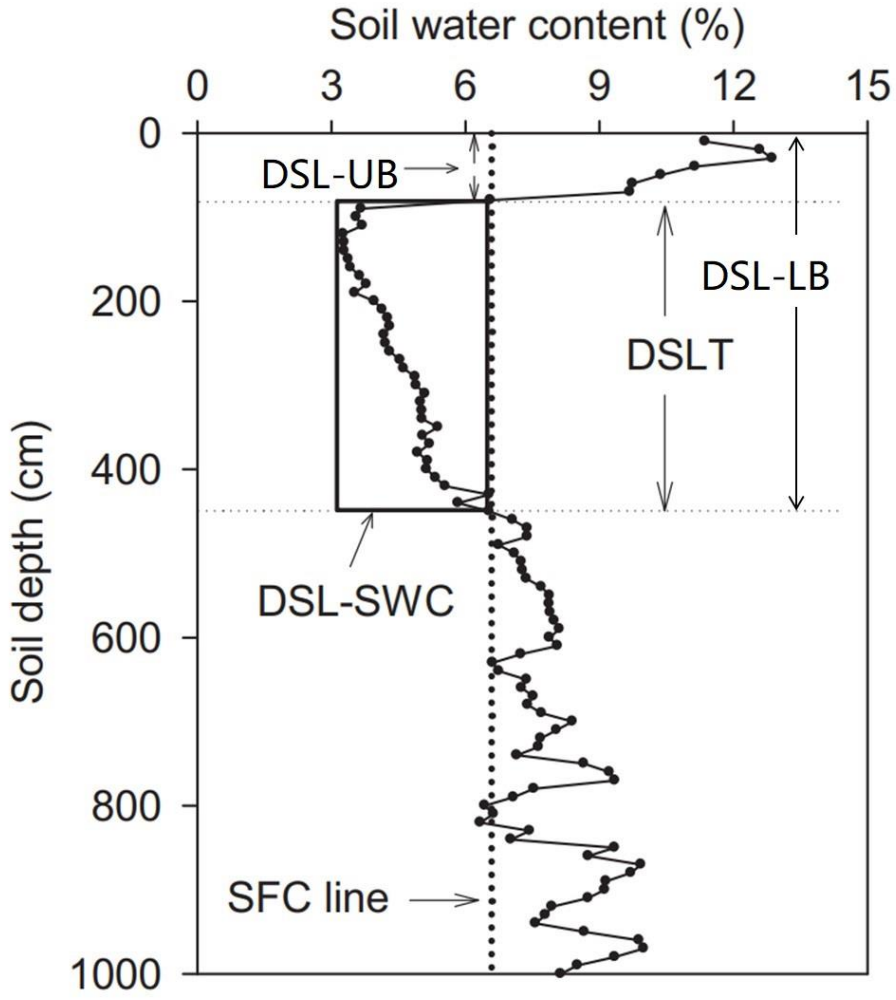

Figure S1: Schematic of the drying soil layer (DSL) evaluation indices in the soil profile: thickness (DSLT), upper boundary (DSL-UB), lower boundary (DSL-LB), mean soil water content (DSL-SWC) and stable field capacity (SFC)). Modified from Fig. 3 in Wang et al. (2011).

3. Model parameters

Table S1 Model Parameters Used in the Simulations.

Variable	Notation	Units	Value	Source
Vegetation Parameters				
Light extinction coefficient	k	-	0.54	Zhang et al., 2015
Plant's minimum temperature for growth	T_b	℃	6	Nietsch et al., 2011
Plant's optimal temperature for growth	T_m	℃	32	Nietsch et al., 2011
Potential heat units required for maturity	**PHU**	℃	2300	Nietsch et al., 2011
Maximum radiation-use efficiency	RUE_{max}	kg MJ^{-1}	2	Nietsch et al., 2011
Maximum leaf area index	LAI_{max}	-	4	Calibrated
Soil water availability of semi-porous conductance	h_{REW}	-	0.3	Sun et al., 2011
Water stress function shape coefficient	k_{REW}	-	6	Sun et al., 2011
Coarse root density	ρ	g cm^{-3}	0.6	Danjon et al., 2013
Cross-sectional area of tap root required for unit fine root	k_A	cm^2 g^{-1}	0.05	derived from pot experiment
Minimum cross-sectional area of coarse root required for extension	A_{min}	cm^2	0.04	Calibrated
Soil Hydraulic Properties				
Exponent of soil-water characteristic curve	*B*	-	8, 6, 8, 7.5, 7, 8, 8, 9, 9, 9, 7.5, 8.5, 9, 7.5	Calibrated
Saturated hydraulic conductivity	K_{sat}	cm h^{-1}	1, 0.8, 0.8, 0.7, 0.7, 0.5, 0.5, 0.5, 0.3, 0.3, 0.2, 0.2, 0.2, 0.2	Calibrated
Model Layers				
Number of layers in the observed root zone (upper 5 m)			100	
Layer thickness of the observed root zone (cm)			5	
Number of layers in the thick unsaturated zone (5 to 20 m)			300	
Layer thickness of the thick unsaturated zone (cm)			5	

In order to determine the value of k_A, the cross-sectional area of coarse roots required for unit fine root ($cm^2\ g^{-1}$), of black locust we also carried pot experiment in 2016. We planted the seedlings of black locust on the pot (with height of 100 cm and diameter of 20 cm) from April and collected 12 pot samples on October. From every pot root sample, two root branch segments have been selected, and each root branch were cut into 6 to 10 pieces for scanning (Perfection v1650, Seiko Epson, Inc., Nagano, Japan). The scanned root images were then processed to distinguish as the fine roots (diameter < 2 mm) and coarse roots (diameter > 2 mm). Then, the value of k_A of 0.05 was derived (shown in **Fig S2**).

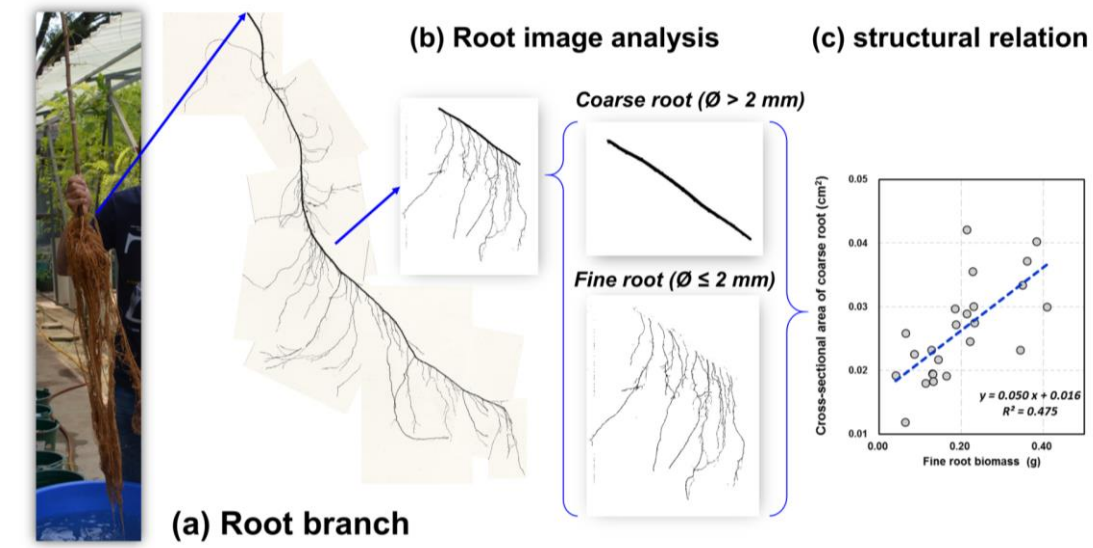

Figure S2: (a) Composite picture of one root branch sample of black locust scanning image from the pot experiment; (b) Distinguishing coarse roots and fine roots based on root diameter by image analysis; (c) structural relation between coarse root cross-sectional area and its attached fine root biomass

4. Supporting simulation results

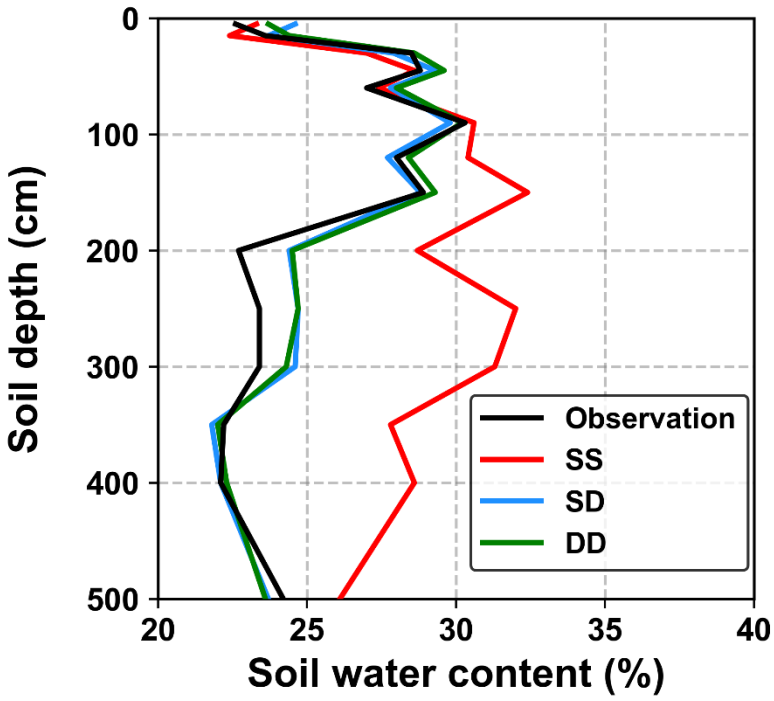

Figure S3: Comparisons of soil water content (SWC, %) of observation and simulation from three approached at various soil depths. The results indicated SD overestimated the SWC in deep soil layers (below 1 m). Notes: SS, Static rooting depth and Static fine root distribution; SD, Static rooting depth and Dynamic fine root distribution; DD, Dynamic rooting depth and Dynamic distribution of fine roots.

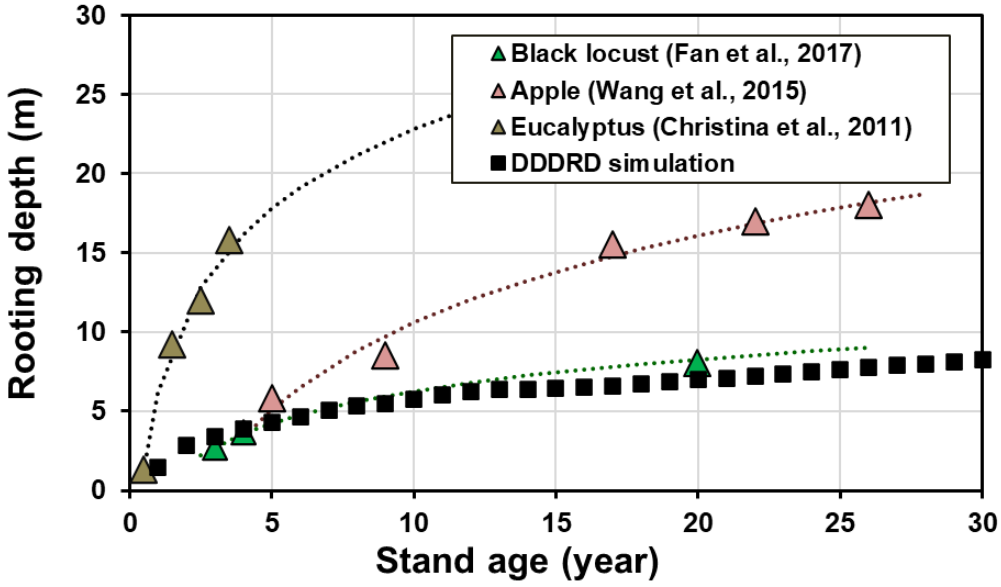

Figure S4: Comparison of yearly rooting depth extension pattern from literature data (triangles) and the simulation (squares). The dotted lines indicated the logarithmic fitting of literature data.

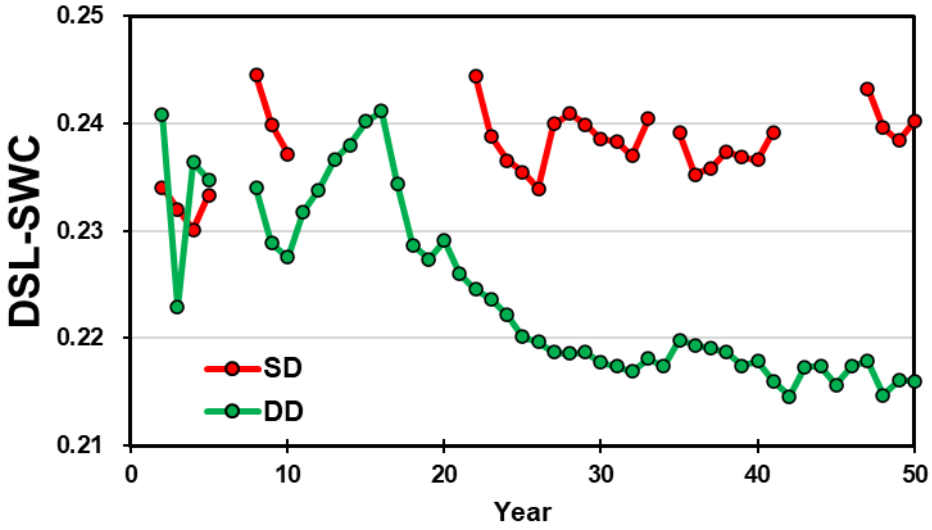

Figure S5: Comparison of dynamics of yearly average DSL-SWC from different approaches (SD and DD approaches).

References

Allen, R. et al.: Crop Evapotranspiration: Guidelines for Computing Crop Water Requirements, FAO Irrigation and Drainage Paper 56, 1998.

Campbell, G.S.: A Simple Method for Determining Unsaturated Conductivity From Moisture Retention Data. Soil Sciences, 117(6), 311-314, doi:10.1097/00010694-197406000-00001, 1974.

Cao, Y., Zhao, Z., Qu, M., Cheng, X.R. and D.H., W.: Effects of *Robinia pseudoacacia* roots on deep soil moisture status, Chinese Journal of Applied Ecology, 17(5), 765-768, 2006 (in Chinese with English abstract).

Chen, W.Q., Li, P. and Zhang, L.E.: Researches on fine root dynamics in *Robinia pseudoacacia* forest and its response with soil moisture, Research of Soil and Water Conservation, 16(6), 92-101, 2009 (in Chinese with English abstract).

Clapp, R.B. and Hornberger, G.M.: Empirical equations for some soil hydraulic properties， Water Resour. Res., 14(4), 601-604, doi:10.1029/WR014i004p00601, 1978.

Danjon, F., Khuder, H. and Stokes, A.: Deep Phenotyping of Coarse Root Architecture in R. pseudoacacia Reveals That Tree Root System Plasticity Is Confined within Its Architectural Model, PLoS One, 8(12), 1-15, doi: 10.1371/journal.pone.0083548, 2013.

Fan, Y., Miguez-Macho, G., Jobbagy, E.G., Jackson, R.B. and Otero-Casal, C.: Hydrologic regulation of plant rooting depth. P. Natl. Acad. Sci. USA, 114(40), 10572-10577, doi:10.1073/pnas.1712381114, 2017.

Hu, X.N. et al.: A Model for Fine Root Growth of *Robinia pseudoacacia* in the Loess Plateau, Scientia Silvae Sinicae, 46(4), 126-132, 2010 (in Chinese with English abstract).

Jia, X.X., Shao, M.A., Zhu, Y.J. and Luo, Y.: Soil moisture decline due to afforestation across the Loess Plateau, China, J. Hydrol., 546, 113-122, doi:10.1016/j.jhydrol.2017.01.011, 2017.

Li, J., Chen, B., Li, X., Zhao, Y., Ciren, Y., and Jiang, B., et al.: Effects of deep soil desiccation on artificial forestlands in different vegetation zones on the Loess Plateau of China, Acta Ecologica Sinica,

28(4), 1429-1445, doi:10.1016/S1872-2032(08)60052-9, 2008.

Li, P., Zhao, Z., Li, Z.B. and Wang, N.J.: Research on root distribution parameters of *Robinia pseudoacacia* on different sites in Chunhua County, Journal of Nanjing Forestry University (Natural Sciences Edition), 26(5), 32-36, 2002 (in Chinese with English abstract).

Li, P., Zhao, Z., Li, Z.B. and Zhan, T.Z.: Characters of root biomass spatial distribution of *Robinia pseudoacacia* in Weibei loess areas, Ecology and Environment, 14(3), 405-409, 2005(in Chinese with English abstract).

Neitsch, S.L., Arnold, J.G., Kiniry, J.R. and Williams, J.R.: Soil and Water Assessment Tool: Theoretical Documentation—Version 2009. Texas Water Resources Institute Technical Report No. 406. Agricultural Research Service (USDA) & Texas Agricultural Experiment Station, Texas A&M University, Temple, 2011.

Oleson, K. et al.: Technical description of version 4.5 of the Community Land Model (CLM), UCAR/NCAR, doi:10.5065/D6RR1W7M, 2013.

Richards, L.A.,: Capillary conduction of liquids through porous mediums. Physics-a Journal of General and Applied Physics, 1(1), 318-333, doi:10.1063/1.1745010, 1931.

Shao, Y. and Irannejad, P.: On the Choice of Soil Hydraulic Models in Land-Surface Schemes, Bound.-Layer Meteor., 90(1), 83-115, doi:10.1023/A:1001786023282, 1999.

Simunek, J. and Hopmans, J.W.: Modeling compensated root water and nutrient uptake, Ecol. Model., 220(4), 505-521, doi:10.1016/j.ecolmodel.2008.11.004, 2009.

Sun, L., Guan, W., Wang, Y., Xu, L. and Xiong, W.: Simulations of Larix principis-rupprechtii stand mean canopy stomatal conductance and its responses to environmental factors, Chin. J. Plant Ecol., 30(10), 2122-2128, doi:10.3724/SP.J.1258.2011.00411, 2011.

Wang, Y. , Shao, M. , Zhu, Y. , and Liu, Z.: Impacts of land use and plant characteristics on dried soil layers in different climatic regions on the loess plateau of china, Agric. For. Meteorol., 151(4), 437-448, doi:10.1016/j.agrformet.2010.11.016, 2011.

Williams, J., Jones, C., Kiniry, J. and Spanel, D.: The EPIC Crop Growth Model, Trans. ASABE, 32(2), 497-0511, doi:10.13031/2013.31032, 1989.

Wu, W., Li, H., Feng, H., Si, B., Chen, G., Meng, T., Li, Y. and Siddique, K.: Precipitation dominates the transpiration of both the economic forest (Malus pumila) and ecological forest (*Robinia pseudoacacia*) on the Loess Plateau after about 15 years of water depletion in deep soil, Agric. For. Meteorol., 297, 108244, doi:10.1016/j.agrformet.2020.108244, 2021.

Xue, W.P., Zhao, Z., Li, P. and Cao, Y.: Researches on root distribution characteristics of *Robinia pseudoacacia* stand in Wangdonggou on different site conditions, Jour. of North west Sci-Tech Univ. of Agri. and For. (Nat. Sci. Ed.), 31(6), 27-32, 2003 (in Chinese with English abstract).

Yang, Y., Donohue, R. and McVicar, T.: Global estimation of effective plant rooting depth: Implications for hydrological modeling, Water Resour. Res., 52(10), 8260-8276, doi:10.1002/2016WR019392, 2016.

Zeng, X. and Decker, M.: Improving the Numerical Solution of Soil Moisture-Based Richards Equation for Land Models with a Deep or Shallow Water Table, J. Hydrometeorol., 10(1), 308-319, doi:10.1175/2008JHM1011.1, 2009.

Zhang, Y., Huang, M. and Lian, J.: Spatial distributions of optimal plant coverage for the dominant tree and shrub species along a precipitation gradient on the central Loess Plateau, Agric. For. Meteorol., 206, 69-84, 2015, doi: 10.1016/j.agrformet.2015.03.001, 2015.

Zhang, Z., Huang, M. and Zhang, Y.: Vertical distribution of fine-root area in relation to stand age

and environmental factors in black locust (*Robinia pseudoacacia*) forests of the Chinese Loess Plateau, Can. J. For. Res., 48(10), 1148-1158, doi:10.1139/cjfr-2018-0149, 2018.

Zhao, Z., Li, P. and Wang, N.J.: Study on relations of growth and vertical distribution of fine root system of main planting tree species to soil density in the Weibei Loess Plateau, Scientia Silvae Sinicae, 40(5), 50-55, 2004 (in Chinese with English abstract).